Surface site density, silicic acid retention and transport properties of compacted magnetite powder

C. Mayant, B. Grambow, Abdesselam Abdelouas, S. Ribet, S. Leclercq

▶ To cite this version:

HAL Id: in2p3-00339559
http://hal.in2p3.fr/in2p3-00339559

Submitted on 24 Nov 2008

Surface site density, silicic acid retention and transport properties of compacted magnetite powder

C. Mayant[1], B. Grambow[1], A. Abdelouas[1], S. Ribet[1] and S. Leclercq[2],

[1] Laboratoire SUBATECH, 4 rue A. Kastler, BP 20722, 44307 Nantes cedex 03, France

[2] Electricité de France, Research and Development, Les Renardières, Route de Sens-Ecuelles, 77818 Moret sur Loing cedex, France

Abstract

In France, within the framework of investigations of the feasibility of deep geological disposal of high-level radioactive waste, studies on corrosion products of steel over packs are ongoing. Such studies concern silica and radionuclide retention. The objective of the present work is to study sorption of silicic acid on compacted magnetite in percolation cells to attempt to simulate confined site conditions. Potentiometric titration of commercial magnetite was carried out with both dispersed and compacted magnetite. The titration of the magnetite suspension has been made with two different methods: a batch method (several suspensions) and a direct fast method (one suspension). The Gran's function gave 1.7 ($\pm$ 0.4) and 2.4 ($\pm$ 0.5) sorption sites.nm^{-2} with these respective methods but site densities as high as 20/nm^2 could be obtained by modelling. The titration of magnetite compacted at 120 bars showed that the evolution of charge density on magnetite surfaces is similar for compacted and dispersed magnetite. Silicic acid sorption onto dispersed and compacted magnetite was similar with sorption site densities ranging between 2.2 and 4.4/nm^2.

Keywords: magnetite; sorption; titration; sites density; advection-dispersion.

Introduction

In France, the concept of deep geological disposal of vitrified high-level radioactive waste includes the steel canister with the nuclear glass surrounded by an iron overpack. In contact with groundwater and repository rock the iron overpack is expected to corrode in confined space into highly compacted corrosion products including magnetite (Fe_3O_4) and siderite ($FeCO_3$). These corrosion products may play a key role in radionuclide retention

via sorption, reduction and precipitation processes. Also, they may enhance glass dissolution via sorption of silicon resulting from glass leaching. Ferrand et al. (Ferrand et al. 2006) showed that under saturation conditions the dissolution rate of the simulated French nuclear waste glass SON 68 increases with decreasing Si-concentration in solution.

In literature many studies are focussed on dispersed magnetite in batch systems, and more precisely on the titration of magnetite and adsorption phenomena (Catalette et al. (1998), Jordan et al. (2007), Marmier and Fromage (2000), Marmier et al. (1999), Martínez et al. (2006), Missana et al. (2003), Philippini et al. (2006), Shen et al. (1999)). The magnetite titrations were made with a surface to volume ratio of 35 m^2/L by Wesolowski et al. (2000), 36 m^2/L for the titrations of Marmier et al. (1999) and of Catalette et al. (1998), 17 m^2/L for the titration of Missana et al. (2003). None of these works concern compacted magnetite. Philippini (Philippini et al. (2006)) studied the sorption of Si on a variety of iron corrosion products including magnetite and siderite in batch systems (in NaCl or in $NaClO_4$ as aqueous solution) with a specific surface area of 1.8 $m^2.g^{-1}$ and obtained a total site density of 6.7 sites per nm^2 and they found a sorption capacity of magnetite with respect to Si of 1.9×10^{-5} $mol_{Si}.g^{-1}_{magnetite}$ (6.4 $sites_{Si}.nm^{-2}$). According to these authors, silica sorption reached a maximum value between pH 7 and 9. Jordan (Jordan et al. (2007)) studied sorption of H_4SiO_4 on iron oxyhydroxides (goethite, hematite and magnetite): for an aqueous silicon concentration of 1.85×10^{-4} M at pH 7 and a mass of solid to solution volume ratio m/V of 20 $g.L^{-1}$ they found a sorption distribution coefficient K_d of 20-28 $mL.g^{-1}$ for both magnetite (1.6 $m^2.g^{-1}$) and hematite (6.0 $m^2.g^{-1}$) and a much higher K_d of 1960 $mL.g^{-1}$ for goethite (45.0 $m^2.g^{-1}$). They successfully described sorption of Si to surface complex formation $\equiv FeH_3SiO_4$ and $\equiv FeH_2SiO_4^-$.

Different approaches have been used to estimate the surface site densities of iron oxides. Lützenkirchen et al. (2002) have studied the limitations of the potentiometric titration technique. They showed that proton active surface density (PASD) is underestimated by continuous titration with strong acids and that apparent PASD values depends on electrolyte concentration and composition. In agreement with the MUSIC model it was suggested to use site densities calculated from crystallographic information for modelling purposes. Wesolowski et al. (2000) have predicted the density of proton active sites on the magnetite surface according to the proton binding constants at 25.0°C for the (111), (100) and (110) faces: this density is obtained at 2.46×10^{-5} $mol.m^{-2}$ (14.8 sites per nm^2), 2.85×10^{-5} $mol \cdot m^{-2}$ (17.2 sites per nm^2) and 4.54×10^{-5} $mol \cdot m^{-2}$ (27.3 sites per nm^2), for theses respective faces.

In the deep geological repository, iron containers will corrode in confined space under mechanical constraints leading to formation of possibly fissured dense corrosion product layers of phases such as magnetite and siderite. Specific surface areas, grain boundary porosity and accessible site densities for these products are not known. In the present work we attempt to approach this situation by studying retention properties of compacted magnetite powder by studying advective transport of reactants in magnetite filled percolation cells. It has been shown by Scheidegger at al. (1994) that advective transport of acid and base and pH breakthrough curves in columns filled with materials of known pH depending charging behaviour can be described mathematically to assess transport in porous media.

The objectives of the present work were 1) to compare the surface properties of dispersed and compacted magnetite, 2) to study silicic acid adsorption on both dispersed and compacted magnetite and 3) to determine some hydrodynamic properties of magnetite compacted in a percolation cell.

Material and methods

1- Magnetite characterization

The commercial magnetite (Fe_3O_4) is the Puratronic® powder provided by Alfar Aesar. The specific surface area has been determined by the Brunauer-Emmet-Teller (BET) method with N_2 adsorption: 1.9 ($\pm$ 0.1) $m^2.g^{-1}$. The solid has been characterized by SEM (scanning electron microscopy) for magnetite powder and for compacted magnetite, by XRD (X-Ray diffraction) for magnetite powder. The SEM images show that magnetite remains porous after compacting the powder. XRD diffractogram is given in Fig 1 showing a nearly pure magnetite with some traces of hematite, α-Fe_2O_3 (less than 2 %).

A point of zero zeta potential (PZZP) was determined by zeta potential measurements of magnetite suspensions in 0.01M NaCl at different pH in contact with air, and found to be 5.2. This value is lower than most of the literature PZC values for magnetite: 5.55 (Catalette et al. (1998)), 6.3 (Marmier et al. (1999)), 7.1 (Missana et al. (2003)). This low value may be caused by CO_2 presence acidifying the solution or by the easy sedimentation of this magnetite powder. Thus, in our case at pH higher than 5.2 the commercial magnetite would have an overall negatively charged surface.
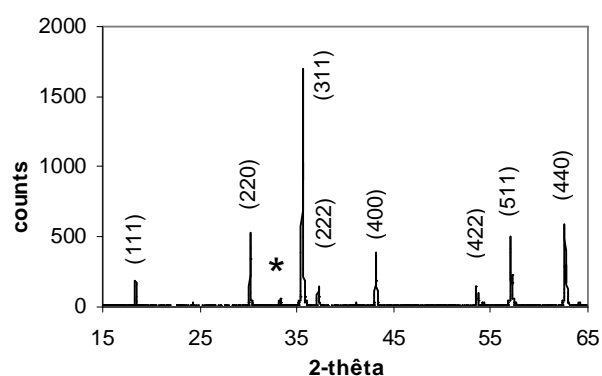
Fig 1: Characterization of the commercial magnetite: X-ray diffraction (SIEMENS D5000, filtration of fluorescence of Fe, Magnetite : JCPDS 00-019-062) *: trace of hematite 01-089-0599)..

2- Acid-base titrations of magnetite suspensions

The titration of the magnetite suspension has been made with two different methods: a batch method and a continuous fast method.

The batch method was conducted at room temperature in a glove box under nitrogen atmosphere at 22.0°C with several suspensions of magnetite (30 g/L, thus 57 m^2 /L) in a 0.01M NaCl electrolytic solution (30 mL). A precise aliquot, different for each suspension, of 0.1M HCl or 0.1M NaOH solutions (which were stored in a glove box) was added in each suspension in order to represent a datum of this titration. The same aliquots of titrant solutions (HCl and NaOH) were added to 0.01M NaCl solution as reference. Equilibration time for suspensions and references was 20 hours under stirring. Then the pH was measured with a PHM220 pHmeter equipped with a combined electrode from Radiometer Analytical. Calibration was done in the pH range 4-9 using standard buffer solutions. In the pH ranges 1 to 4 and 9 to 12, calibration was done using as prepared solutions of NaOH or HCl in 0.01 M NaCl with nominal H^+ activities values calculated using either the Davies equation (Davies 1962) or the code PHREEQC (Parkhurst and Appelo (2006)), a computer program for simulating chemical reactions and transport processes in water. Suspensions were filtered by means of membranes of a pore size of 0.2 μm. Dissolved iron was measured by ICP-MS (inductively coupled plasma mass spectrometry) in order to detect magnetite dissolution during the titration process. SEM and EDX analyses before and after titration for some batch experiments have indicated (Fig 2) that, within the uncertainty of the method, the magnetite surface does not change after titration. Thus, no oxidised surface like HFO or Fe_2O_3 was observed after this titration.
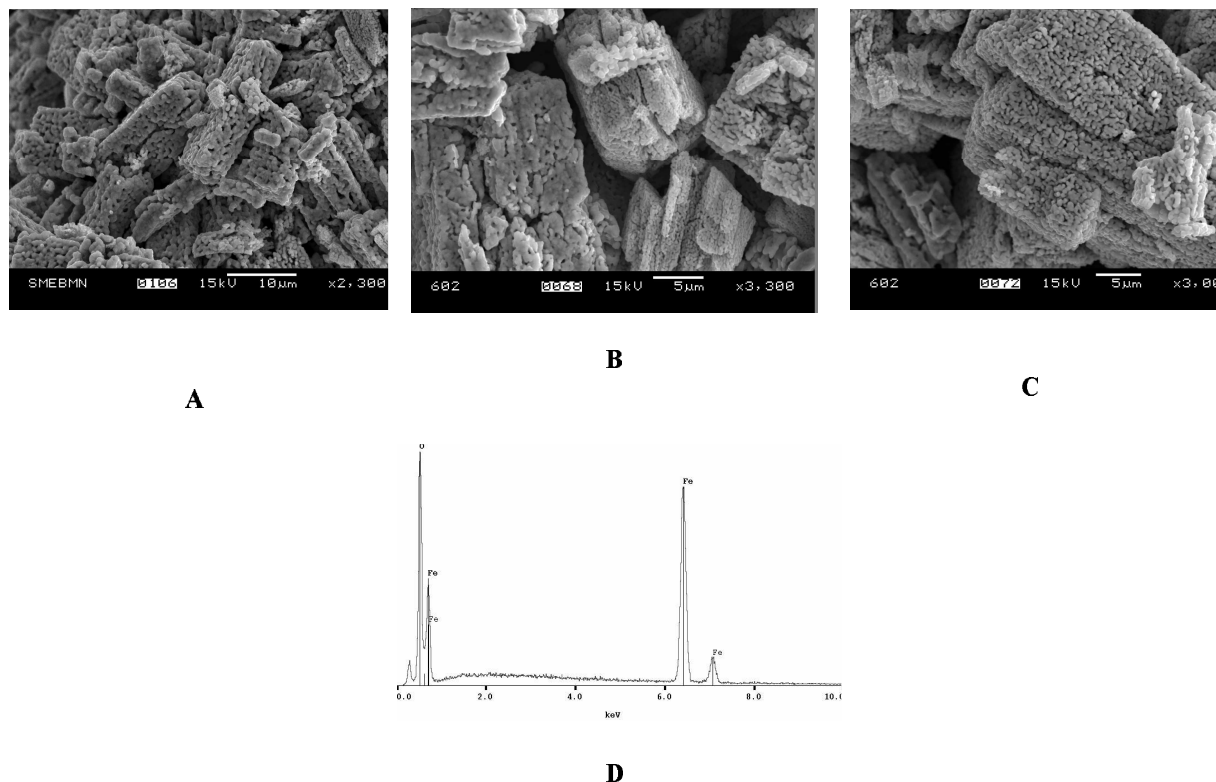
A **B** **C**

D

*Fig 2: Characterization of the commercial magnetite by SEM: **A** before titration; **B** after adding a HCl aliquot for the batch titration; **C** after adding a NaOH aliquot for the batch titration; **D** microanalysis of these magnetite samples.*

The fast titration method was realized with only one suspension of magnetite (30 g/L) in a 0.01M NaCl electrolytic solution (30 mL). The suspension was continuously flushed with nitrogen to prevent contamination with air. The temperature of the suspension was maintained at 25.0 ($\pm$ 0.3) °C using a thermostatic bath. This suspension was stirred for 20 hours to equilibrate the solid/solution interface prior to starting the experiment. Thereafter titration in acidic direction was done by adding 0.1M HCl until pH 2 was reached; then 0.1M NaOH (which was stored in a vessel under nitrogen flux) was added until pH 12 was reached, with an equilibration time of 120 to 210 seconds between two increments. The titration was carried out with an automatic Metrohm titrator equipped with a combined Metrohm electrode. Aliquots of 100 μL of titrant were added when the pH variations were small between two increments, and smaller volumes of titrant (3 μL) were added when the pH variations were important. Total solution volume was then 39.9 mL. The same experiment was made with 0.01M NaCl solution as reference. Due to the added HCl and NaOH volumes the final ionic strength increased from initially 10^{-2} ,to a maximal value of 2.7×10^{-2}.

3- Silicic acid retention on dispersed magnetite

A stock solution with 1.26×10^{-3}M of silicic acid was prepared by diluting a SCP Science silicon standard of 3.6×10^{-2} M which was stabilised by a HNO_3 matrix. The final pH of the stock solution was adjusted to 7.8 by addition of 0.1M NaOH solution. Then, this silicic acid solution was deoxygenated using a vacuum pump. The absence of polymeric Si species in the stock solution was confirmed by comparing ICP-MS with UV-Vis spectroscopic measurements, the latter responding only to monomer Si as described below.

To provide a base for comparison with compacted magnetite, batch adsorption experiments with dispersed magnetite were conducted in plastic vessels at room temperature in an anaerobic glove box. The magnetite powder was rinsed with a 0.01M NaCl deoxygenated solution. Five batch experiments were prepared by addition of 0.9 g of magnetite powder in 30 mL of the silicic acid stock solution. After an equilibrium time of 50 h, the supernatants were removed and filtrated on 0.2 µm filters.

The monomer silicon concentration was measured by UV-Vis spectrophotometry on a Shimadzu 2401 double beam spectrometer. This UV-Vis method needs 3 reactants. The first reactant is ammonium heptamolybdate (Merck) which is stored in acidic medium (sulfuric acid) and thus forms the hexamolybdenum acid ion: it reacts with silicic acid to form the yellow molybdosilicic acid complex. The second reactant is the tartaric acid (Merck) which reacts with this yellow complex to form the tartrate molybdenic complex. Finally the third reactant is a reducing agent (Merck), which forms the silicomolybdenic blue complex absorbing light at about 820 nm.

A calibration curve was realized with silicon concentration standards in the range 7.1×10^{-6} - 5.1×10^{-5}M, prepared with the SCP Science silicon standard of 3.6×10^{-2} M. Standards and sample solutions were prepared with the 3 reactants and were put in 1 cm-thick cuvettes (in quartz) to be analysed in the wavelength range 400-900 nm. A 0.01M NaCl solution was used as background electrolyte after addition of the 3 reactants.

The stock solution and some representative samples were analysed as well by ICP-MS to quantify the total silicon concentration, and, by comparison to the UV-Vis analyses, to make sure that no silica polymers were formed in the solutions.

The sorption distribution coefficient Kd was determined according to the equation (1):

$$Kd = \frac{[H_4SiO_4]_{solid}}{[H_4SiO_4]_{supernatant}} \times \frac{V}{m} \qquad (1)$$

where $[H_4SiO_4]_{supernatant}$ is the silicic acid concentration in the supernatant after adsorption; $[H_4SiO_4]_{solid}$ the difference between the silicic acid concentration in the stock solution and the silicic acid concentration in the supernatant; V the total volume of the suspension and m the magnetite mass.

4- Hydrodynamic properties and acid base titration of compacted magnetite

30 g of magnetite were compacted with a hydraulic press at about 120 bars in a stainless steel percolation cell. The compacted magnetite cylinder is 4.5 cm in length and 2 cm in diameter leading to a total volume of 14.1 cm^3. After compaction, stainless steel filters were put at both ends of the magnetite cylinder. Weighting the cell before and after saturation by the 0.01M NaCl solution allowed calculating a pore volume of 9.2 cm^3 and a porosity of 65%. This is a much higher porosity than the expected porosity of magnetite formed on container surfaces under geological disposal conditions, but it represents a first step in simulating repository conditions since surface to volume ratios change from about 57 m^2/L in studies with dispersed magnetite to a value of about 6200 m^2/L, provided all surfaces of the compacted magnetite powder remain accessible.

The percolation cell was then connected to a peristaltic pump with a constant flow rate and with an imposed pressure < 2 bars. An inlet stock solution was continuously injected at a side of the magnetite core with the pump and samples were collected in absence of air on the other side of the magnetite core at defined times. The inlet solution was continuously purged with nitrogen which was purified from oxygen by passing through an ammonium metavanadate solution containing Zn(Hg) amalgam.

Prior to experiments the compacted magnetite was rinsed with a 0.01M NaCl solution: the peristaltic pump was delivering a constant flux of an inlet stock solution of 0.01M NaCl (pH 7.5) until the outlet pH matched the inlet one. The initial pH of the outflowing solution was 4.6 and the overall volume pumped through compacted magnetite to reach the final pH of 7.5 was 533 mL. The collected outlet samples were analysed by ICP-MS for dissolved iron.

Hydrodynamic properties of the compacted magnetite column were studied by subsequently injecting a tritiated solution. Tritium has no or little sorption affinity with solid surface (García-Gutiérrez et al. (2004), Van Loon et al. (2003)). As inlet solution a tritiated 0.01M NaCl solution was used with an activity of 300 Bq/L. Each collected sample was weighted at defined time intervals allowing determination the exact flow rate.

Tritium was measured with a Canberra liquid scintillation apparatus. This experiment was stopped when the tritium concentration in the collected samples equalized that in the inlet stock solution.

After removal of the remaining tritium by flushing with a 0.01M NaCl solution, the acid/base titration of the compacted magnetite surface was realized. The inlet stock solution was no more purged with nitrogen as this experiment was conducted in a glove box filled with argon to prevent magnetite oxidation and carbon dioxide contamination. The flow rate was fixed at 0.29 mL/min. The inlet (titrant) solution was a diluted HCl or NaOH solution of known pH. The titration was realized from initial pH 7 towards pH 11, then back from pH 11 to pH 3, by steps of one pH unit. The pH in the outlet samples, collected at defined time intervals, was recorded: once the pH in the collected samples was the same as the one of the inlet stock solution, this solution was replaced with a solution of another pH. So, from pH 7 to pH 11, the inlet stock solutions are NaOH solutions more and more concentrated; and from pH 11 to pH 3, the inlet stock solutions are first NaOH solutions more and more diluted and then HCl more and more concentrated. Only in the pH range 5 to 6, this procedure was impossible due to the low acid strength and inlet solutions were changed before the target pH was reached. The collected samples with pH <7.5 were analysed by ICP-MS to measure potentially dissolved iron.

5- Silicic acid retention on the compacted magnetite

The silicic acid adsorption was studied in two percolation cells containing compacted magnetite. One of the cells had been used before in the acid/base titration experiment: after titration the magnetite was rinsed another time by 0.01M NaCl until the pH of the outlet solution is about 8. The second column was prepared for the sorption experiments by similar compaction pressure and preequilibration procedure with a 0.01M NaCl solution as described above. The inlet and the outlet solutions were stored in PFA plastic vessels. Stock solutions of silicic acid were prepared by diluting a SCP Science silicon standard solution of 3.6×10^{-2}M: the concentration of the inlet silicic acid stock solution was 4.5×10^{-4}M (case of first column) or 1.6×10^{-3}M (case of second column) with an adjusted pH of 8.5. The solutions were passed through the magnetite columns using the peristaltic pump at 10 μL/min. A daily outlet sample was collected, its pH was measured and its monomer silicon concentration ($[Si]_{outlet}$) was determined by the UV-Vis method as described above. The volume was determined by weighting each collected outlet sample (V_{outlet}).

The sorption distribution coefficient for the silicic acid ($L.g^{-1}$) was determined with the following equation:

$$Kd = \frac{\Sigma \left[(n_{H4SiO4})_{inlet} - (n_{H4SiO4})_{outlet} \right]}{m \times [H_4SiO_4]_{tot}} \qquad (2)$$

with $(n_{H4SiO4})_{outlet}$ is the measured number of moles of monomer silicon in the collected sample volume (V_{outlet}), $(n_{H4SiO4})_{inlet}$ the hypothetical total number of moles of monomer silicon in the collected sample if silicon concentrations would have been at the inlet value, m the magnetite mass (g) and $[H_4SiO_4]_{tot}$ the silicon concentration in the inlet stock solution (mol/L). For each collected sample, $(n_{Si})_{inlet}$ and $(n_{Si})_{outlet}$ are calculated as following:

$$(n_{H4SiO4})_{outlet} = [H_4SiO_4]_{outlet} \times V_{outlet} \qquad (3)$$

$$(n_{H4SiO4})_{inlet} = [H_4SiO_4]_{tot} \times V_{outlet} \qquad (4)$$

The number of active surface sites for silicic acid sorption was determined with the equation (5):

$$N_{H4SiO4} = \frac{\Sigma \left[(n_{H4SiO4})_{inlet} - (n_{H4SiO4})_{outlet} \right] \times N_A}{m \times S \times 10^{18}} \qquad (5)$$

where N_A is the Avogadro number; m the magnetite mass (g); and S the specific surface area ($m^2.g^{-1}$) of the magnetite powder prior to compaction.

At test termination, the desorption of silicic acid from the magnetite surface was studied on the two percolation cells with a 0.01M NaCl solution as inlet solution.

6- Determination of the surface site concentration

To determine the surface site concentration of the dispersed magnetite, the Gran's function was used (Michel (2005), Prélot (2001)):

$$F_1 = (V_{in} + V_{added}) \times 10^{-pH}, \text{ for pH} < 7.0 \qquad (6)$$

$$F_2 = (V_{in} + V_{added}) \times 10^{pH + \log Kw}, \text{ for pH} > 7.0 \qquad (7)$$

where V_{in} is the initial volume (30 mL) and V_{added} is the added volume in the reactor at the considered pH. K_w is the ionic product of water at a given temperature and a given ionic strength: for the batch titration $\log K_w$ is considered to be $-14,02$ (T= 22.0 °C) and for the direct fast titration it is considered to be $-13,93$ (T= 25.0°C), according to PHREEQC calculations for these respective temperatures. The plot of the Gran's function versus the added volume of titrant can be fitted by two straight lines that cross the x-axis at V1 and V2. The surface site concentration (sites.nm^{-2}) is then calculated according to:

$$N_{sites} = \frac{C_{titrant} \times (V2 - V1) \times N_A}{m \times S \times 10^{18}} \tag{8}$$

where $C_{titrant}$ is the concentration of the titrant solution (0.1M), N_A the Avogadro number, m the magnetite mass (g) and S its specific surface area (m^2.g^{-1}).

Surface charge densities Q (in moles/m^2) during fast and batch titration of dispersed magnetite as well as for compacted magnetite during potentiometric percolation tests were calculated using the following formulas for the titration of dispersed magnetite:

$$Q = \left(\frac{[HCl] \cdot V_{HCl,add} - ([OH^-]_{init} - [H^+]_{init}) \cdot V_{init}}{V_{init} + V_{HCl,add}} + [OH^-]_{fin} - [H^+]_{fin} \right) \Big/ S \tag{9a}$$

$$\tag{9 b}$$

$$Q = \left(-\frac{[NaOH] \cdot V_{NaOH,add} - ([OH^-]_{init} - [H^+]_{init}) \cdot V_{init}}{V_{init} + V_{NaOH,add}} + [OH^-]_{fin} - [H^+]_{fin} \right) \Big/ S$$

Where [NaOH] and [HCl] are the molar concentrations of the titrant, V_{init}, $V_{HCl,\ add}$ and $V_{NaOHadd}$ are the volumes of the initial solutions and of the aliquot of added HCl or NaOH, S is the ratio of the magnetite surface to the solution volume in units of m^2/L , [OH]$_{init}$, [OH]$_{fin}$, [H$^+$]$_{init}$ and [H$^+$]$_{fin}$ are the molar concentrations of OH$^-$ and H$^+$ ions derived from the measured pH in the initial and final solutions considerant K_W and the activity coefficient of H$^+$ in the solution calculated, using the Davis equation. Corrections for dissolution of Fe^{2+} during batch titration in the pH range 2 to 5 is considred modifying Eq. 9 to

$$Q = \left(\frac{[HCl] \cdot V_{HCl,add} - ([OH^-]_{init} - [H^+]_{init}) \cdot V_{init}}{V_{init} + V_{HCl,add}} - 2 \cdot [Fe^{2+}] + [OH^-]_{fin} - [H^+]_{fin} \right) \Big/ S \tag{9c}$$

For titration of the compacted magnetite with n percolating volumes of either acid ($\Delta V_{HCl,add,n}$) or base $\Delta V_{NaOH,add,n}$ these equations transform to

$$Q = \sum_n \left(-\frac{[NaOH]_n \cdot \Delta V_{NaOH,add,n} - [HCl]_n \cdot \Delta V_{HCl,add,n}}{V_{init} + V_{NaOH,add,n} + V_{HCl,add,n}} + [OH^-]_n - [H^+]_n - 2[Fe^{2+}] \right) \Big/ S \tag{9d}$$

the volumes of acid added become zero in case of titration with base and vice versa. The formula takes into account the steps of the titration with titrant solutions of different concentrations and the correction by Fe dissolution (see table 2 further below). The specific surface area of the magnetite was assumed to be the same in the compacted state as in the powder state.

7- Modelling

The geochemical code PHREEQC was used to model the experimental data concerning titrations and transport phenomenon inside the compacted magnetite. The version of PHREEQC (version 2) includes ion-exchange equilibria, solid-solution equilibria, advective transport, diffusion or dispersion in 1D transport. The diffuse layer model was used: near the surface of the solid, the first layer contains specifically adsorbed ions, and farther the surface, a diffuse layer contains ions which balance the surface charge. The solid is assumed to have hydroxyl groups at the surface that can be protonated or deprotonated according to the following equations:

$$\text{Magn-OH} + \text{H}^+ \leftrightarrow \text{Magn-OH}_2^+ \qquad\qquad\qquad \log Ka_1 \qquad\qquad (10)$$

$$\text{Magn-O}^- + \text{H}^+ \leftrightarrow \text{Magn-OH} \qquad\qquad\qquad \log Ka_2 \qquad\qquad (11)$$

According to Blesa et al. (1984), Missana et al. (2003), and Philippini et al. (2006), $\log Ka_1$ values range between -3.87 and -5.1 and $\log Ka_2$ values are between -8.26 and -9.10.

PHREEQC allow 1D transport calculation according to the advection-reaction-dispersion (ARD) equation (Parkhurst and Appelo (2006)):

$$\frac{\partial C}{\partial T} = -v\frac{\partial C}{\partial x} + D_L\frac{\partial^2 C}{\partial x^2} - \frac{\partial q}{\partial t} \qquad\qquad (12)$$

where the first term represents the advection, second term is the dispersion and the third term is the change in concentration in the solid phase due to reaction. In this study the last term is not considered as the concentration in the solid phase (q) does not change. D_L is the apparent hydrodynamic dispersion coefficient $(m^2.s^{-1})$ in the pore water accessible for diffusion, v the apparent advection velocity $(m.s^{-1})$, x position, t time and C concentration for the injected tracer or titrant in the diffusion accessible pore water of the solid. D_L is described as follow:

$$D_L = D_e + \alpha_L.v \qquad\qquad (13)$$

with D_e the effective diffusion coefficient $(m^2.s^{-1})$ and α_L the dispersivity (m): D_L represents the molecular diffusion (first term) and the mechanical dispersion (second term).

Results and discussion

1- Acid-base titrations of magnetite suspensions

The results of both fast and batch titration are first interpreted using the Gran's function (equations (6) and (7)). Results are shown for the fast titration in Fig 3 as function of the volume of added NaOH during the backward titration (from pH 2 to pH 12). The sites density is calculated with the equation (8) using the V1 and V2 volumes, determined as 1.831 (±0.009) and 1.905 (± 0.019) mL, respectively by linear regression analyses. The number of proton active sites obtained with the fast titration method is then 2.4 (± 0.5) sites.nm^{-2}.
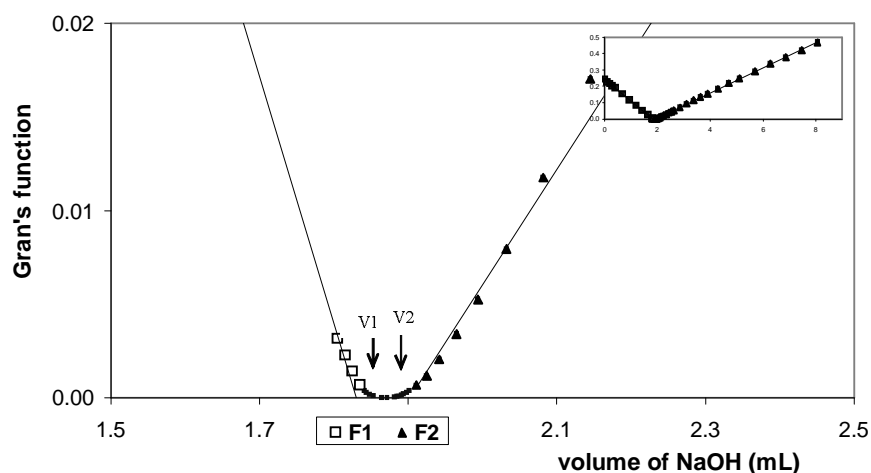

Fig 3: Fast titration of the dispersed magnetite (30 g/L) in 0.01 M NaCl solution from pH 2 to pH 12; Zoom of the Gran's function,, where (o) represents the linear Gran's function F1 to obtain V1 and (▲) the linear Gran's function F2 to obtain V2.

For batch titration, the obtained V1 and V2 volumes are very small (less than 0.05 mL for both V1 and V2). In this case the surface site concentration obtained is 1.7 (± 0.4) sites.nm^{-2} without correction of magnetite dissolution.

A small fraction of the magnetite surface may have been transformed into Fe_2O_3 in acidic medium according to:

$$[Fe^{II}Fe_2^{III}]O_4 + 2H^+ \rightarrow [Fe_2^{III}]O_3 + Fe^{2+} + H_2O \qquad (14)$$

So, iron analysis allowed to take into account proton consumption via magnetite dissolution in acidic solutions using equation (14) (White and Peterson (1996), White et al. (1994)). The results of protons consumption due to magnetite dissolution and Fe^{2+} release in acidic solutions are shown in Fig. 4. The lower the pH, the higher was the proton consumption.

The minimum PASD is 2.1 ($\pm$ 0.5) sites.nm^{-2} after the magnetite dissolution correction and by using:

$$N_{sites} = \frac{([H^+]_{adsorbed} - [H^+]_{consumed}) \times V \times N_A}{m \times S \times 10^{18}} \tag{15}$$

where $[H^+]_{adsorbed}$ is the proton concentration which is accessible at the magnetite surface (mol/L); $[H^+]_{consumed}$ is the proton concentration which is consumed during the magnetite dissolution and V the total volume of the magnetite suspension (L).

The minimum PASD of magnetite is similar for both fast and batch methods and is consistent with the literature data (Catalette et al. (1998), Marmier et al. (1999), Missana et al. (2003), Philippini et al. (2006), Shen et al. (1999)).
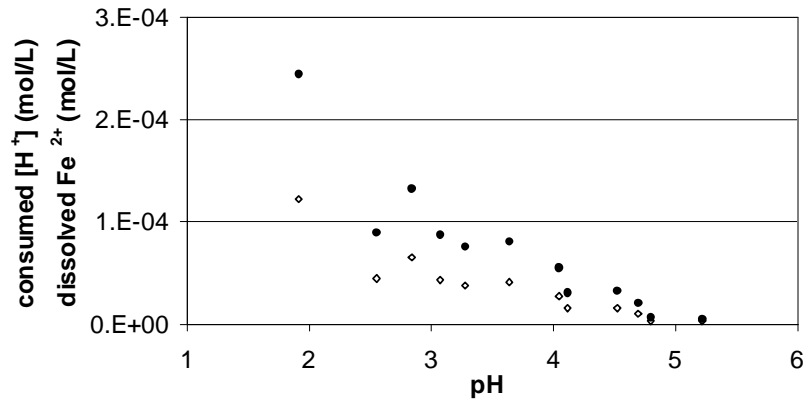

Fig. 4: ($\bullet$) H^+ consumption and ($\Diamond$) Fe^{2+} release attributed to magnetite dissolution during batch titration.

Experimentally determined surface charge densities in fast and batch titrations as well as in percolation tests with compacted magnetite have been simulated with PHREEQC (Fig. 5). The fitting parameters were Ka_1 and Ka_2 constants (equations ((10) and (11)) and the number of sites. In the range of pH 5 to 12, obtained Ka_2 values and site densities were found correlated. Site densities could be fitted with values between 2 and 20 depending to

the weight given to the data between pH 11 and 12. It shall be mentioned that the data in the pH range 11-12 are rather uncertain since in this pH range small errors in pH measurement of either percolating or calibrating solution or of temperature will have large effects on the calculated surface charge. Due to this uncertainty a site density of $20/nm^2$ has arbitrarily been selected, consistent with the average crystallographic site density (Wesolowski et al. 2000). Average values of pKa_1 of $5.8(\pm0.3)$ and pKa_2 of $7.8(\pm0.7)$ were obtained with the diffuse double layer model. In general the curves obtained in the present work for dispersed magnetite are rather similar within the experimental scatter to literature data published by Wesolowski et al. (2000).
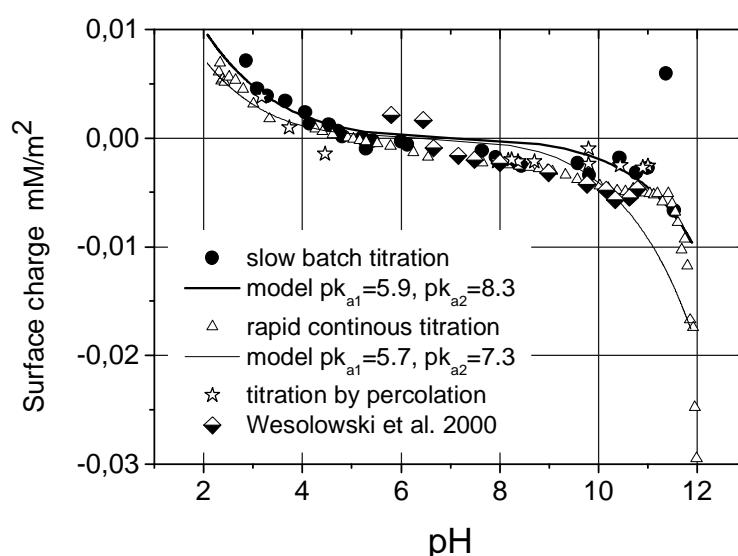

Fig. 5: Surface charge densities calculated with Eqs. 9 both for rapid and batch titration of dispersed magnetite, for compacted magnetite. Comparison to literature data and model curves (PHREEQC).

Both the initial presence of less than 2% of Fe_2O_3 and the leaching of Fe^{2+} according to Eq. 14 might have influenced our titration results. Formation of goethite can be ruled out as it has not been observed by SEM after reaction and it would have a much larger specific surface area than those observed in the present study. The agreement of the present data with those of Wesolowski et al. (2000) for pure magnetite (without traces of Fe_2O_3) indicates that the effect of Fe_2O_3 on our results may not be very important.

2- Silicic acid retention on the dispersed magnetite

Silica polymers were not formed in the silicic acid samples as the concentrations obtained by ICP-MS were the same as the monomer silicon concentrations obtained by the UV-Vis method.

At pH 7.8, 18 % of the silicic acid was adsorbed on the magnetite surface leading to a final Si concelntration of 1.03 mM. The sorption distribution coefficient K_d has been determined with the equation (1): the average K_d for the five batches is 7 ($\pm$ 1) mL·g^{-1}. The formal number of sites adsorbing H_4SiO_4 on the magnetite surface was determined using equation (15) by replacing C with the total silicic acid concentration, which is adsorbed on the overall magnetite surface. A value of H_4SiO_4 2.2 ($\pm$ 0.2) sites per nm^2 (7.0×10^{-6} $mol_{H4SiO4}.g^{-1}_{magnetite}$) was obtained, which is consistent with the surface site density obtained by Gran's titration: the minimum PASD is also accessible to the silicic acid on the dispersed magnetite surface. These values may be compared to literature data. Our results are lower than the mean value but still in the error margin of the maximal sorption values reported by Philippini et al. (2006) of 19 ($\pm$ 14) $\times 10^{-6}$ $mol_{Si}.g^{-1}_{magnetite}$ at pH 8.5 corresponding to sorption sites densities for dispersed magnetite with respect to total dissolved Si of 6.4 $sites_{Si}.nm^{-2}$. From the author's Figure 3 a K_d value of 20 mL.g^{-1} or 12 mL·g^{-1} can be obtained for H_4SiO_4 concentration < 0.4 mM or 1 mM respectively . K_d values reported by Jordan et al. (2007) of 20 mL.g^{-1} (m/V = 55 g.L^{-1}) or 28 mL.g^{-1} (m/V =40 g.L^{-1}) for maximum H_4SiO_4 concentrations < 0.2 mM were similar to those of Philippini et al. (2006).

3- Compacted magnetite

3.1- Hydrodynamic study

The breakthrough curve (Fig 6) obtained with the tritiated solution shows that the advection is the most important transport phenomenon; diffusion process can be neglected. It is consistent with the observation that our compacted commercial magnetite has a great permeability. Modelling of the breakthrough curve with PHREEQC resulted in α_L = 5×10^{-3} m and D_e < 10^{-10} $m^2.s^{-1}$. D_e is close to zero and diffusion is negligible compared to advective transport.
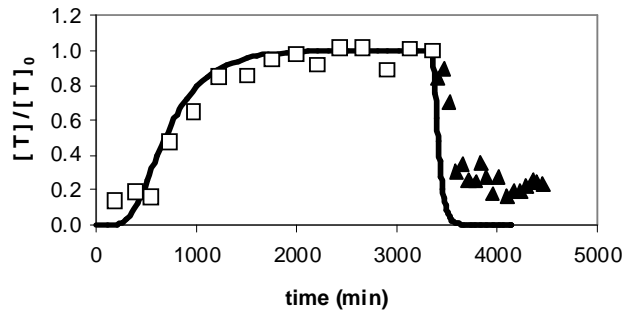
Fig 6: Breakthrough curve of tritiated solution in magnetite column: (□) experimental data for the tritium percolation; (▲) experimental data obtained from washing with NaCl solution; (solid line) calculated curve; [T] / [T]$_0$ is the ratio between the tritium concentration in the collected outlet sample and the tritium concentration in the inlet stock solution.

With a fixed flow rate of 0.010 mL/min and a porous volume of 9.2 mL, the percolation time is 15h. Then apparent hydrodynamic dispersion coefficient (D$_L$) can be determined with the equation (11) as 4.2 ($\pm$ 0.1) $\times 10^{-9}$ m^2.s^{-1}. The Péclet number is 9 at 0.010 mL /min and about 300 at 0.33 mL /min. This indicates that titration data are essentially advection dominated.

3.2- Titration

The titration of the compacted commercial magnetite is realized in order to assess the effect of compaction on the surface charge density. Table 1 gives the volumes, concentrations and pH (inlet) of the percolated titrants as well as the pH of the outlet solutions just before the titrant has been changed. It can be seen that titrants with an inlet pH between 5 and 6 were unable to significantly changing the outlet pH. The backward titration down to pH 3 required a correction of proton consumption according to Eq. 9d due to magnetite dissolution based on Eq 14. Some typical data for Fe concentrations measured in outlet solutions are given in table 2. The calculated (Eq. 9d) total surface charge density has been included in Fig. 5. The similarity of the curves for titration of dispersed and compacted magnetite indicates that site densities and surface acidity constants are rather similar for dispersed and compacted material. Obviously, the commercial magnetite used in the present work does not loose sorption sites upon compaction. Our titration method of the compacted state was efficient to obtain reliable data.

added titrant	NaOH					HCl					
$C_{titrant}$ ($\times 10^4$ mol/L)	3.98	1.15	0.13	0.05	0.01	0.03	0.09	0.71	0.62	4.55	9.44
V_{outlet} (mL)	148	215	398	198	949	361	996	392	926	569	320
pH inlet	10.5	10.0	9.0	8.7	8.0	6.0	5.3	5.0	4.3	3.5	3.0
pH outlet	10.54	9.90	8.96	8.70	8.44	8.00	8.25	8.30	4.30	3.60	3.00

Table 1: Concentration and volume of added titrant for each range of pH during the step by step backward titration (from pH 11 to pH 3) of the 30 g-compacted magnetite. The value "pH outlet" correspond to the pH in the outlet solution just before changing the titrant (pH inlet)

measured pH	dissolved Fe by ICP-MS ($\times 10^6$ mol /L)	consumed [H$^+$] ($\times 10^6$ mol /L)
7.42	1.09	2.18
4.37	4.19	8.38
4.16	95.20	190.30
3.50	36.20	72.40
3.59	343.20	686.40
2.92	65.50	131.00

Table 2: Iron and equivalent consumed [H+] concentrations due to magnetite dissolution in typical samples collected in the acid/base percolation tests with compacted magnetit. Data for the step by step backward titration (from pH 11 to pH 3) of the 30 g-compacted magnetite. Measurements were only performed for pH<7.5

The pH values in the outlet solution volumes collected during titration of the compacted magnetite with the various percolating solutions is shown in Figure 7 as a function of total percolated solution volume. The results are compared with model curves calculated with PHREEQC using the hydrodynamic parameters from the percolation experiment with tritium and the acid base constants and site densities used to fit surface charge densities of dispersed magnetite (Figure 5). The direct application of the model data from figure 5 did not give a very good representation of the experimental results. The model could be improved significantly after changing the site density from 20 to 0.5/nm^2. Further improvement will depend on improving the acid base model used in figure 5.
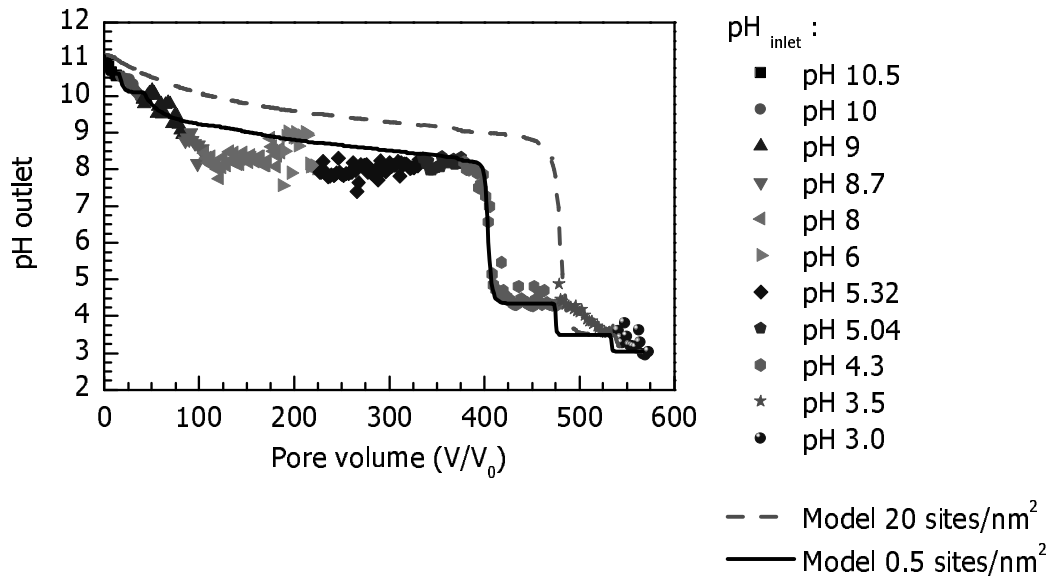
Figure 7 : Results for compacted magnetite of percolation with acid and base titrants (compositions given in table 1). Comparison is made with two model curves using hydrodynamic data from percolation with tritium and surface acidity constants determined for the data in figure 5 and a site density of either 0.5 or 20/nm²

3.3- Silicic acid adsorption and desorption

The results of H_4SiO_4 sorption on compacted magnetite at pH 8 are given in Fig. 8. Final solution concentrations are about 90 to 95% of the initial value indicating close to equilibrium conditions for the distribution coefficients and very little concentration gradients of Si in the percolation reactor. The determined K_d (equation 2) is 16 mL.g^{-1} for the sorption experiment with 4.5×10^{-4} M H_4SiO_4 and 9 mL.g^{-1} for the experiment using 1.6×10^{-3} M H_4SiO_4. Compacted magnetite adsorbed about 7.0×10^{-6} $mol_{H4SiO4}.g^{-1}_{magnetite}$ (2.2 ($\pm$ 0.2) $sites_{H4SiO4}.nm^{-2}$, according to equation (5)) for the 4.5×10^{-4} M experiment, and 1.4×10^{-5} $mol_{H4SiO4}.g^{-1}_{magnetite}$ (4.4 ($\pm$ 0.4) $sites_{H4SiO4}.nm^{-2}$) for the 1.6×10^{-3} M experiment. Thus, the first experiment leads to the same density of accessible sorption sites (2.2 ($\pm$ 0.2) $sites_{H4SiO4}.nm^{-2}$) than the experiment of Si sorption on the dispersed magnetite, and thus confirms that magnetite does not loose accessible surface sites when compacted at 120 bars.
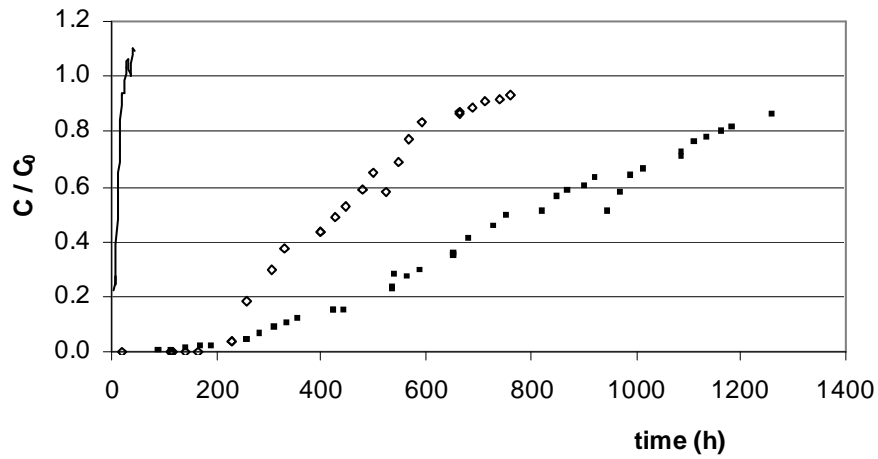
Fig 8: Silicic acid adsorption on the compacted magnetite at pH 8 with an inlet stock solution of (■) 4.5×10⁻⁴M; (◊) 1.6×10⁻³M. Comparison with the transfer of the tritiated solution (solid line) in the percolation cell containing compacted magnetit.
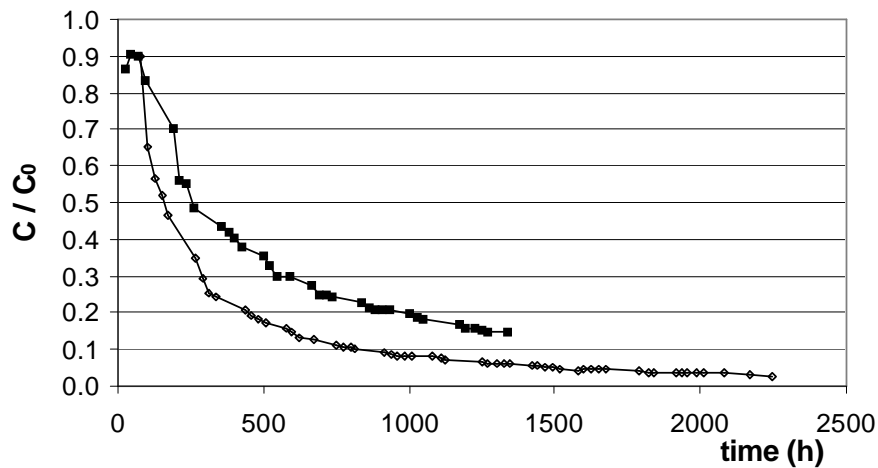

Fig 9: Silicic acid desorption by flushing the compacted magnetite column with 0.01M NaCl. Results are given for columns loaded in the initial sorption experiment with an inlet stock solution for the adsorption of H_4SiO_4 of (■) 4.5×10⁻⁴M; (◊) 1.6×10⁻³M.

Moreover, this surface site occupation is similar to the minimum PASD obtained for the acid base titrations of the dispersed magnetite. This suggests that all proton accessible sites are also accessible to the silicic acid. The second experiment leads to a number of sites of 4.4 sites$_{H4SiO4}$.nm^{-2}, more close to the maximum sorption values reported by Philippini et al. (2006). This confirms that the actual surface site density is larger than the

minimum one determined for proton active sites by the Gran's plot (Fig. 3). A comparison of present results with literature data obtained in the pH range 7 to 8.5 is given in Fig. 10. This plot confirms that the data for compacted magnetite follow the general trend of sorption data obtained for dispersed systems. From this data it is not clear whether saturation of sorption sites is already obtained for highest H_4SiO_4 concentrations.
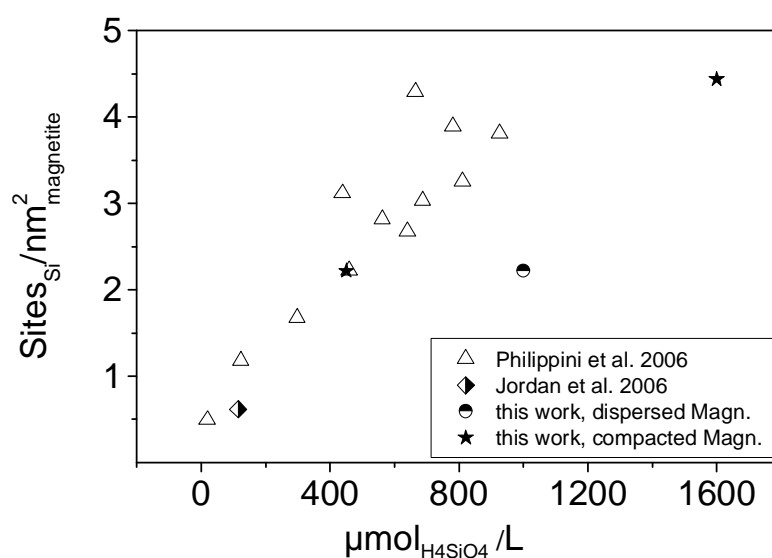

Fig. 10: Sorption isotherm for H4SiO4 on compacted and dispersed magnetite in the pH range 7 to 8.5. Comparison of data from this work with literature data. Data of Philippini et al. 2006 were obtained from the Figure 3 of the authors, data of Jordan et al. 2007 from the Figure 2 of the authors.

The reversibility of silicic acid uptake on compacted magnetite has been studied with the two percolation cells. Fig 9 shows the silicic acid desorption from the magnetite surface. The first experiment with an inlet stock solution of silicic acid of 4.5×10^{-4}M has been stopped in order to characterize the magnetite surface with adsorbed silicic acid: 58 % of adsorbed silicic acid has then been desorbed. For the second experiment, 73 % of adsorbed silicic acid has been desorbed after 2200 hours.

Conclusions

New methods for measuring acid base and retention properties of compacted magnetite have been developed. The titration of the magnetite suspension has been made with two different methods: a batch method (several suspensions) and a direct fast method (one suspension). The Gran's function gave a minimum PASD of 1.7 to 2.4 sites per nm^2 with these respective methods. Similar surface charge densities were found for dispersed

and compacted magnetite. This indicates that commercial magnetite did not loose surface site upon compaction. The modelling with PHREEQC, correcting for Fe^{2+} dissolution gave a value of pKa_1 of 5.8($\pm$0.3) and a pKa_2 value of 7.8($\pm$0.7) with a site density of $20/nm^2$ used from crystallographic data. Site densities and pKa_2 values were found to be highly correlated and data could even be fitted with site densities as low as $1.9/nm^2$.

The results of modelling the percolation test of titrants in compacted magnetite indicate that PASD might have been reduced during compaction but considering the uncertainty in the obtained site densities, such conclusion cannot yet been drawn. This is particularly true since the observed charge densities are rather similar for compacted and dispersed material (Fig. 5).

For an initial H_4SiO_4-concentration in solution of $4.5\times10^{-4}M$ compacted magnetite sorbed 7.0×10^{-6} $mol_{H4SiO4}.g^{-1}_{magnetite}$ (2.2 $sites_{H4SiO4}.nm^{-2}$) at pH 8, corresponding to a Kd of 16 mL/g. This is very similar to the minimum PASD obtained by Gran's functions and very similar to the H_4SiO_4-sorption sites density at pH 8 on the dispersed magnetite. The larger sorption site density of 4.4 $sites_{H4SiO4}.nm^{-2}$ observed for the higher H_4SiO_4 concentration ($1.6\times10^{-3}M$) are a further indication that more surface sites are available for Si sorption than those obtained by Gran's functions.

References

Blesa, M. A., Figliolia, N. M., Maroto, A. J. G., Regazzoni, A. E., 1984. The influence of temperature on the interface magnetite-aqueous electrolyte solution.. Journal of Colloid and Interface Science, 101, 410-418.

Catalette, H., Dumonceau, J., Ollar, P., 1998. Sorption of cesium, barium and europium on magnetite. Journal of Contaminant Hydrology, 35, 151-159.

Davies, C.W. 1962. Ion association. Butterworths, London.

Ferrand, K., Abdelouas, A., Grambow, B., 2006. Water diffusion in the simulated French nuclear waste glass SON 68 contacting silica rich solutions: Experimental and modeling. Journal of Nuclear Materials, 355, 54-67.

García-Gutiérrez, M., Cormenzana, J. L,. Missana T., and Mingarro M. 2004. Diffusion coefficients and accessible porosity for HTO and ^{36}Cl in compacted FEBEX bentonite, Applied Clay Science, 26, 65-73.

Jordan, N., Marmier, N., Lomenech, C., Giffaut, E., Ehrhardt, J., 2007. Sorption of silicates on goethite, hematite, and magnetite: Experiments and modelling. Journal of Colloid and Interface Science, 312, 224-229.

Lützenkirchen, J., Boily J-F., Lövgren, L., Sjöberg, S., 2002. Limitations of the potentiometric titration technique in determining the proton active site density of goethite surfaces. Geochimica et Cosmochimica Acta. 66, 3389-3396.

Marmier, N., Delisée, A., Fromage, F., 1999. Surface complexation codeling of Yb(III), Ni(II), and Cs(I) sorption on magnetite. Journal of Colloid and Interface Science, 211, 54-60.

Marmier, N. and Fromage, F., 2000. Sorption of Cs(I) on magnetite in the presence of silicates. Journal of Colloid and Interface Science, 223, 83-88.

Martínez, M., Giménez, J., de Pablo, J., Rovira, M., Duro, L., 2006. Sorption of selenium(IV) and selenium(VI) onto magnetite. Applied Surface Science, 252, 3767-3773.

Michel, N., 2005. Étude de la solubilité des oxydes et oxohydroxydes de zirconium caractérisés. Ph. D. Thesis; Université de Nantes, Nantes (France), 197p.

Missana, T., García-Gutiérrez, M., Fernńdez, V., 2003. Uranium (VI) sorption on colloidal magnetite under anoxic environment: experimental study and surface complexation modelling. Geochimica et Cosmochimica Acta, 67, 2543-2550.

Parkhurst, D. L. and Appelo, C. A. J., 2006. PHREEQC, a computer program for speciation, batch-reaction, one dimensional transport, and inverse geochemical calculations. version 2.12.

Philippini, V., Naveau, A., Catalette, H., Leclercq, S., 2006. Sorption of silicon on magnetite and other corrosion products of iron. Journal of Nuclear Materials, 348, 60-69.

Prélot, B., 2001. Mesure et modélisation de l'hétérogénéité énergétique à l'interface oxyde/ électrolyte/ métaux. Ph. D. Thesis, Institut National Polytechnique de Lorraine.

Scheidegger, A., Bürgisser, C.S., Borkovec, M., and Sticher, H., 1994. Convective transport of acids and bases in porous media. Water resources research, 30, 2937-2944.

Shen, J., Ebner, A. D., Ritter, J. A., 1999. Points of zero charge and intrinsic equilibrium constants of silica–magnetite composite oxides. Journal of Colloid and Interface Science, 214, 333-343.

Van Loon, L. R., J. M. Soler, and M. H. Bradbury 2003, Diffusion of HTO, $^{36}Cl^-$ and $^{125}I^-$ in Opalinus Clay samples from Mont Terri: Effect of confining pressure, Journal of Contaminant Hydrology, 61, 73-83.

Wesolowski, D. J., Machesky, M. L., Palmer, D. A., Anovitz, L.M., 2000. Magnetite surface charge studies to 290°C from in situ pH titrations. Chemical Geology, 167, 193-229.

White, A. F. and Peterson, M. L., 1996. Reduction of aqueous transition metal species on the surfaces of Fe(II) -containing oxides. Geochimica et Cosmochimica Acta, 60, 3799-3814.

White, A. F., Peterson, M. L., Hochella, M. F., 1994. Electrochemistry and dissolution kinetics of magnetite and ilmenite. Geochimica et Cosmochimica Acta, 58, 1859-1875.